

Estimating and Reducing Uncertainty in Reverberation-Chamber Characterization at Millimeter-Wave Frequencies

Damir Senic, *Member, IEEE*, Kate A. Remley, *Fellow, IEEE*, Chih-Ming Jack Wang, Dylan F. Williams, *Fellow, IEEE*, Christopher L. Holloway, *Fellow, IEEE*, Diogo C. Ribeiro, *Student Member, IEEE*, and Ansgar T. Kirk

Abstract—This contribution provides techniques for accurately characterizing uncertainty when measuring total radiated power (TRP) at millimeter-wave frequencies. The setup is based on the reverberation chamber as a well-known measurement environment capable of performing TRP measurements of wireless devices. We show that by applying various stirring techniques, we can reduce the random component of measurement uncertainty to around 2%. We use a model for estimating the uncertainty for TRP measurements based on the K factor, which is compared with uncertainties calculated from relative power measurements and we show excellent agreement. We perform a significance test to confirm that the uncertainty due to the limited number of mode-stirred samples dominates over the uncertainty due to the lack of spatial uniformity. The observed uncertainty is also compared with an ideal chamber situation and shows good agreement.

Index Terms—Measurement uncertainty, millimeter wave, reverberation chamber (RC), total radiated power (TRP), wireless systems.

I. INTRODUCTION

REVERBERATION chambers (RCs) are well established as an alternative to more expensive anechoic chambers for performing various electromagnetic measurements [1]–[7], including radiated immunity, radiated emissions, shielding effectiveness, antenna efficiency, probe calibration, and material properties characterization. Recently, their use as

Manuscript received September 25, 2015; revised April 12, 2016; accepted April 17, 2016. Date of publication April 20, 2016; date of current version July 5, 2016.

D. Senic is with the Communications Technology Laboratory, National Institute of Standards and Technology, University of Colorado at Boulder, Boulder, CO 80305 USA (e-mail: damir.senic@nist.gov).

K. A. Remley, D. F. Williams, and C. L. Holloway are with the Communications Technology Laboratory, National Institute of Standards and Technology, Boulder, CO 80305 USA (e-mail: kate.remley@nist.gov; dylan.williams@nist.gov; christopher.holloway@nist.gov).

C.-M. J. Wang is with the Statistical Engineering Division, National Institute of Standards and Technology, Boulder, CO 80305 USA (e-mail: chih-ming.wang@nist.gov).

D. C. Ribeiro was with Electromagnetics Division, National Institute of Standards and Technology, Boulder, CO 80305 USA. He is now with the Telecommunications Institute (IT), University of Aveiro, 1049 - 001 Lisboa, Portugal. (e-mail: diogo.ribeiro@nist.gov).

A. T. Kirk was with the Electromagnetics Division, National Institute of Standards and Technology, Boulder, CO 80305 USA. He is now with the Institute of Electrical Engineering and Measurement Technology, Leibniz Universität Hannover, Hannover 30167, Germany (e-mail: kirk@geml.uni-hannover.de).

Color versions of one or more of the figures in this paper are available online at <http://ieeexplore.ieee.org>.

Digital Object Identifier 10.1109/TAP.2016.2556711

measurement environments in the wireless community has become increasingly popular [8]–[12]. Various wireless applications include total radiated power (TRP), receiver sensitivity, and throughput measurements. Recently, wireless applications have experienced immense growth in both indoor and outdoor environments. Hence, wireless-system manufacturers demand an adaptive, reliable, and controllable measurement facility capable of replicating these real-world environments for device testing. According to [13]–[17], RCs prove to be a suitable choice capable of simulating multipath environments.

An RC can be regarded as an electrically large resonator with a high- Q value [2], [18]. Due to that fact, the instantaneous spatial distribution of the electromagnetic fields inside such an environment is not uniform. In order to estimate a quantity of interest from measurements in an RC, we need to average over measured randomized field samples. Some common stirring techniques used to statistically randomize the fields inside a chamber include mechanical paddle stirring and antenna position stirring. In the former, electrically large paddle(s) move and change the boundary conditions inside a chamber. In the latter, an antenna is moved inside the chamber's working volume, sometimes also accompanied by changing the antenna's polarization.

Much of the prior work on uncertainty in RC measurements can be found in [10]–[12] and [19]–[21]. In the uncertainty study in [10], an empirical model for the uncertainty of the over-the-air (OTA) measurements was proposed. The model was based on the average K factor and was said to be valid for any value of K factor. A somewhat different approach proposed in [11] was based on a components-of-variance in a model. The model utilized, in this paper, focuses on a setup with a very low- K factor in order to achieve very low uncertainty.

A few studies dealing with the RC behavior at millimeter-wave frequencies have been published. Dielectric conductivity and permittivity tests in the 30–40-GHz range performed in a cylindrical RC were given in [22]. Emission tests of different electrical components from 1 to 40 GHz have been performed in [23]. In [24], the design and experimental validation of an RC up to 61.5 GHz was presented. Since this frequency range will be used in the next-generation high-speed wireless networks [25], thorough study of RC performance at millimeter-wave frequencies is of great importance.

Even though communication at millimeter-wave frequencies will make use of the line-of-sight (LoS) component, we still see a significant scattered (diffuse) field [26] in non-LoS conditions. In TRP OTA tests, the focus is on power measurements averaged over different stirrer orientations, as opposed to simulation of a multipath channel.

Here, we present a guide for the evaluation of the uncertainty in the RC at millimeter-wave frequencies that was not performed so far. Low uncertainty is especially important in the millimeter-wave frequency range due to the fact that the required measurement accuracy linearly increases with frequency, because a phase error linearly increases with frequency.

In this paper, we perform a significance test [12], [27] to compare two different components of uncertainty: 1) the uncertainty due to the finite number of mode-stirred measurement samples, which originates within a given mode-stirring sequence and 2) the uncertainty due to the lack of spatial uniformity of the averaged fields in the chamber, which originates between different antenna locations in the chamber. By applying the significance test, we show that the uncertainty due to the finite number of mode-stirred measurement samples is dominant, as expected, because spatial uniformity is high in our unloaded chamber.

We present an evaluation of measurement uncertainty that can be used for Continuous Wave TRP measurements inside an unloaded RC at millimeter-wave frequencies. Modulated-signal measurements are more involved and will be left for future research. The goal of this paper is to reduce the random component of measurement uncertainty to as low value as possible, preferably close to 2%. To achieve such a low uncertainty, a large number of mode-stirred samples are necessary, along with highly automated measurements.

This paper provides two significant contributions that were not previously published: 1) detailed measurement uncertainty evaluation at millimeter-wave frequencies and 2) a rigorous step-by-step guide for the evaluation of RCs as common measurement facilities in the wireless communications and Electromagnetic Compatibility.

The outline of this paper is as follows. A model for measurement uncertainty based on a low value of Rician K factor for TRP measurements is given in Section II. Section III follows with a detailed explanation of our measurement setup and techniques used to evaluate the measurement uncertainty for RC-based TRP measurements. Since very low- K factor values are of utmost importance for such low measurement uncertainty, we also present, in this section, helpful techniques for lowering the K factor. Section IV summarizes the parameters necessary to configure the RC in order to achieve such low uncertainty. It also gives a detailed study on K factor as a key parameter for our uncertainty evaluation. Measurement results and their comparison with the proposed model for uncertainty due to a finite number of mode-stirred samples in a mode-stirring sequence from a significance test are given in Section V. The final conclusions can be found in Section VI. The results of the significance test are given in the Appendix.

II. ESTIMATING MEASUREMENT UNCERTAINTY OF TOTAL RADIATED POWER IN A REVERBERATION CHAMBER

The objective of this paper is to determine measurement uncertainty associated with total power radiated by a device under test (DUT). In order to determine the power radiated by the DUT, it is necessary to determine the chamber's reference power transfer function $\langle G_{\text{REF}} \rangle_{N,M,F}$, averaged over F frequencies, N stirrer orientations, and M antenna positions, as measured by a measurement antenna whose efficiency (e_{MEAS}) is known.

As in [12], we define average received power as

$$\begin{aligned} \langle P_{\text{REC,DUT}} \rangle_{N,M,F} &= \frac{P_{\text{RAD,DUT}} e_{\text{MEAS}} \langle G_{\text{DUT}} \rangle_{N,M,F} (1 - |\Gamma_{\text{MEAS}}|^2)}{|1 - \Gamma_{\text{MEAS}} \Gamma_{\text{RX}}|^2} \quad (1) \end{aligned}$$

where $P_{\text{RAD,DUT}}$ is the power radiated by the DUT antenna, $\langle G_{\text{DUT}} \rangle_{N,M,F}$ is the chamber's power transfer function, Γ_{RX} is the reflection coefficient of the receiver assembly, and Γ_{MEAS} equals the free-space reflection coefficient of the measurement antenna. In practice, Γ_{MEAS} is commonly approximated from a measurement of $\langle S_{22,\text{REF}} \rangle_{N,M,F}$, which is determined during reference measurements. The term $(1 - |\Gamma_{\text{MEAS}}|^2)$ corresponds to the measurement antenna impedance mismatch. Equation (1) was originally derived in [12, Appendix A]. The product, $\Gamma_{\text{MEAS}} \Gamma_{\text{RX}}$, in (1) comes from the reflections at the measurement antenna port (Γ_{MEAS}) and the reflections at the receiver assembly port (Γ_{RX}). In prior work [6], these were combined in a single term.

The power radiated by the DUT can then be written as

$$P_{\text{RAD,DUT}} = \frac{\langle P_{\text{REC,DUT}} \rangle_{N,M,F} |1 - \Gamma_{\text{MEAS}} \Gamma_{\text{RX}}|^2}{e_{\text{MEAS}} \langle G_{\text{DUT}} \rangle_{N,M,F} (1 - |\Gamma_{\text{MEAS}}|^2)}. \quad (2)$$

The chamber's power transfer function in the case of DUT measurements is commonly estimated from the chamber's reference power transfer function. Even though the DUT antenna will not identically excite the chamber as does the reference antenna, common practice is to assume that the reference antenna has similar radiation characteristics to the DUT from a radiation pattern point of view. If the K factors of both the DUT and reference measurements are sufficiently low and similar, one can assume that $\langle G_{\text{DUT}} \rangle_{N,M,F} \approx \langle G_{\text{REF}} \rangle_{N,M,F}$ [6], [12].

The chamber's reference power transfer function may then be estimated from S-parameter measurements and written as

$$\langle G_{\text{REF}} \rangle_{N,M,F} = \frac{\langle |S_{21,\text{REF}}|^2 \rangle_{N,M,F}}{e_{\text{REF}} e_{\text{MEAS}} (1 - |\Gamma_{\text{REF}}|^2) (1 - |\Gamma_{\text{MEAS}}|^2)}. \quad (3)$$

By combining (3) and (4) and with $\langle G_{\text{DUT}} \rangle_{N,M,F} \approx \langle G_{\text{REF}} \rangle_{N,M,F}$, we obtain an expression for total power radiated by the DUT

$$\begin{aligned} P_{\text{RAD,DUT}} &= \frac{\langle P_{\text{REC,DUT}} \rangle_{N,M,F} |1 - \Gamma_{\text{MEAS}} \Gamma_{\text{RX}}|^2 e_{\text{REF}} (1 - |\Gamma_{\text{REF}}|^2)}{\langle |S_{21,\text{REF}}|^2 \rangle_{N,M,F}} \quad (4) \end{aligned}$$

where the ensemble averages for $\langle |S_{21, \text{REF}}|^2 \rangle_{N, M, F}$ have been performed at F frequency points, N mode-stirred samples (stirrer orientations), and M antenna locations.

Note that the received power at the receiver assembly in (4) is precorrected for known receiver effective efficiency (η_{RX}) and reflection coefficient (Γ_{RX}) [28]

$$\langle P_{\text{REC, DUT}} \rangle_{N, M, F} = \frac{\langle P_{\text{RX}} \rangle}{\eta_{\text{RX}}(1 - |\Gamma_{\text{RX}}|^2)}. \quad (5)$$

For uncorrelated measurements (i.e., negligible correlation between frequencies, paddle orientations, and antenna positions), the uncertainty due to the finite number of mode-stirred samples [given in (A.1)] for the received power measurements at a single antenna location (m_j) may be approximated by [11, eq. (17)], [12]

$$u_{\text{REF}, K}(m_j) = \sqrt{\frac{K^2 + \frac{2K}{N} + \frac{1}{N}}{K^2 + 2K + 1}}. \quad (6)$$

The power at the receive antenna is generally formed out of two components: a stirred component that varies with both the paddle orientations and the antenna position, and an unstirred component that is K times the stirred one where its uncertainty only depends on the antenna position. Therefore, at a single antenna location, averaging over different paddle orientations will only reduce the uncertainty due to the stirred power. On the other hand, the uncertainty due to the unstirred power will remain unaffected by paddle stirring. For small K factor values, this uncertainty contributes less to the total uncertainty, because it is considerably smaller.

In wireless tests, the uncertainty due to the lack of spatial uniformity can play a significant role in total uncertainty, i.e., it can dominate, as compared with the uncertainty due to the finite number of mode-stirred samples [12]. However, this is not always the case. To determine which component of the uncertainty is dominant, a significance test may be performed (see the Appendix). For insignificant spatial uniformity uncertainty, shown in the Appendix, the standard uncertainty can be expressed as

$$u_{\text{REF}} = \sqrt{\frac{\sum_{i=1}^N \sum_{j=1}^M [G_{\text{REF}}(n_i, m_j) - \langle G_{\text{REF}} \rangle_{N, M}]^2}{NM(NM - 1)}} \quad (7)$$

where u implicitly depends on the K factor, since the variability of $G_{\text{REF}}(m_j)$ depends on the unstirred energy in the chamber.

Uncertainties due to both the components (lack of spatial uniformity and finite number of mode-stirred samples) are considered as independent and can be reduced by averaging over different antenna positions M [12].

III. MEASUREMENT SETUP

To illustrate the assessment of uncertainty described in Section II, we performed all the measurements over a frequency range from 43 to 47 GHz using an RC and a 50-GHz Vector Network Analyzer (VNA), as shown in Fig. 1. The chamber was equipped with two mechanical stirrers.



Fig. 1. Measurement setup. Illustration of product names does not imply endorsement by NIST. Other products may work as well or better.

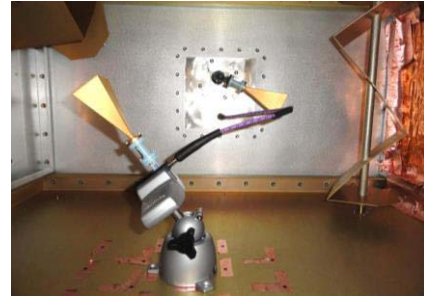


Fig. 2. Antenna orientation inside RC. The WR-22 waveguide bulkhead can be seen at the rear of the chamber while the 2.4-mm coaxial bulkhead is connected, through a cable, to the movable transmit antenna.

The larger one rotated about a horizontal (H) axis within a cylindrical volume of 0.6-m height and 0.2-m diameter, while the smaller one rotated about a vertical (V) axis within a cylindrical volume of 0.5-m height and 0.2-m diameter. The RC's size was 1 m (l) \times 0.65 m (w) \times 0.55 m (h), which corresponds to an electrical size of approximately $150\lambda \times 100\lambda \times 80\lambda$, at the center frequency of 45 GHz. This is important to emphasize, since the high operating frequency results in a large electrical size for the RC, despite its small physical size.

The RC's bulkhead was equipped with two feedthroughs; one waveguide that was connected to VNA's port 2 and one 2.4-mm coaxial connected to VNA's port 1. The waveguide horn receive antenna at port 2 was oriented toward the vertical stirrer (see Fig. 2) and was used as the measurement (receive) antenna. The signal from the 2.4-mm feedthrough was brought to the transmit antenna via a coaxial cable and a coaxial-to-waveguide transition. We used an open-ended waveguide (OEW) as the reference transmit antenna and another waveguide horn antenna as a simulated DUT. The antennae were oriented away from each other in order to lower the unstirred energy (K factor) between them.

There are several different approaches to reduce the coupling between the antennae in the RC. In this paper, we chose the approach based on redirecting the antennae away from each other. Another approach would include placing a shield between the antennae [10]. However, our initial, unpublished studies show little reduction in the K factor, possibly due to the diffractions from the shield at high frequencies. Therefore, we utilized antenna redirection in order to achieve the low- K factor necessary for low uncertainty,

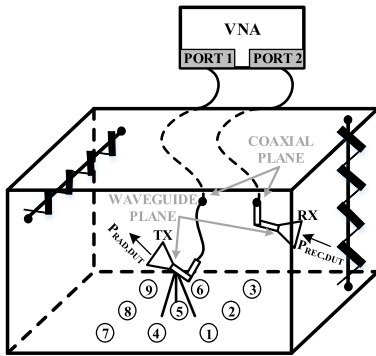


Fig. 3. Schematic of measurement setup showing two different calibration planes and nine antenna locations.

TABLE I
MEASUREMENT PARAMETERS

Parameter	Value	
Frequency range	43 GHz – 47 GHz	
Number of frequency points	1601	
IF bandwidth	Calibration	100 Hz
	Measurements	2 kHz
VNA output power level	-10 dBm	
VNA dwell time	10 μ s	
Paddle step size ($V \times H$)	$3.6^\circ \times 3.6^\circ$	
Number of paddle orientations ($V \times H$)	100 x 100	

which was the goal of this paper. Note that this method does not apply if the antenna has unknown radiation pattern. However, that particular case is beyond the scope of this paper.

The transmit antennae were oriented toward the horizontal stirrer and positioned at nine different locations within the RC's working volume (see Figs. 2 and 3) in order to check the spatial uniformity of the setup. Key measurement parameters are summarized in Table I.

S-parameters were measured for 10000 paddle orientations (100 vertical and 100 horizontal) at each of nine transmit antenna positions. Since each measurement took ~ 24 h, a VNA calibration was performed prior to each change of the antenna position. Calibration standards and DUT measurements were collected as raw data, and a correction was performed afterward within the National Institute of Standards and Technology (NIST) microwave uncertainty framework [29], [30].

A schematic of the measurement setup is shown in Fig. 3, where one can observe two different calibration planes; waveguide at the antenna ports and coaxial at the RC bulkhead ports, where we used a coaxial-to-waveguide adapter. Since the calibration inside the chamber was physically inconvenient, the calibration plane was transformed from waveguide to coaxial plane outside the chamber by embedding the system components through the postprocessor in the uncertainty framework [31].

The calibration measurements were performed before the DUT measurements were started and verified just after they were finished. In Fig. 4, we see the spread of the reflection coefficient (S_{11}) SHORT standard and the spread of the transmission coefficient (S_{21}) THRU standard before and after

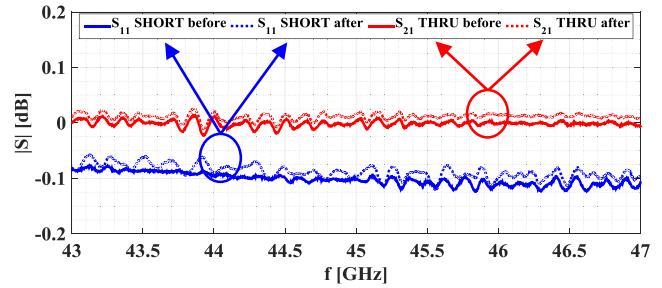


Fig. 4. Spread of reflection and transmission coefficients of SHORT and THRU standards before and after the measurements, approximately 24 h.

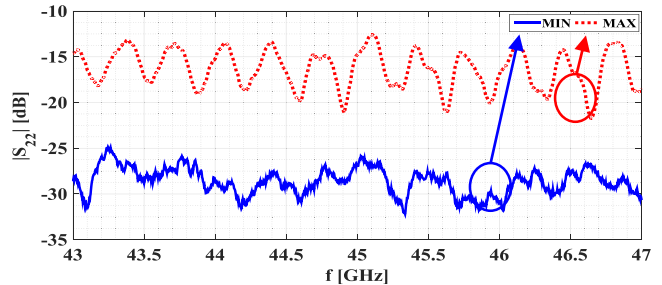


Fig. 5. Spread of the magnitude of S_{22} for horizontal receive antenna without randomized copper plate.

the measurements. The observed calibration deviation in a 24-h period was below 0.025 dB and taken as negligible.

Initially, the receive antenna was horizontally orientated aiming toward the vertical stirrer and side wall behind the vertical stirrer. Those preliminary measurements showed strong specular reflections from the wall behind the stirrer at certain paddle orientations. At some paddle orientations, the stirrer was almost transparent and a large amount of energy was reflected back to the antenna. The magnitude of S_{22} varied as much as 15 dB depending on the paddle orientation. The minimum and maximum magnitudes of the S_{22} -parameter for the horizontally orientated receive antenna are shown in Fig. 5. One can observe highly periodic behavior as a function of frequency. To eliminate these effects, the bulkhead was first rotated, so that the receive antenna was oriented toward the RC's corner, and, additionally, a custom-made copper plate with a randomized surface was placed in front of the RC's side wall behind the vertical stirrer. Both the adaptations can be seen in Fig. 2. The outcome was a significantly reduced spread of $|S_{22}|$ and of the periodic behavior, as shown in Fig. 6.

IV. DETERMINING MEASUREMENT PARAMETERS FOR UNCERTAINTY CALCULATIONS

In order to evaluate the measurement uncertainty associated with a particular RC setup, the number of uncorrelated mode-stirred samples should be determined. In addition, knowledge of the K factor can help refine the estimation of uncertainty for realistic chamber setups [11], [12], [24].

A. Number of Uncorrelated Frequency and Stirrer Samples

The number of uncorrelated frequency samples that can be collected in a certain frequency range, as well as the effective

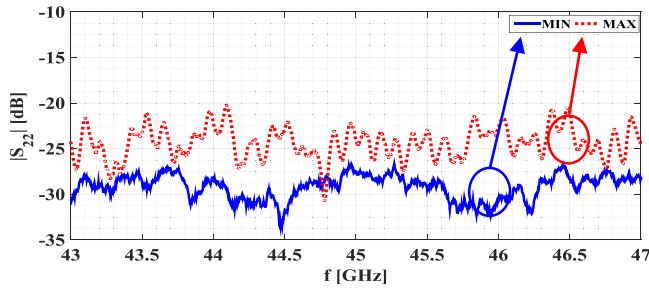


Fig. 6. Spread of the magnitude of S_{22} for reoriented receive antenna with randomized copper plate.

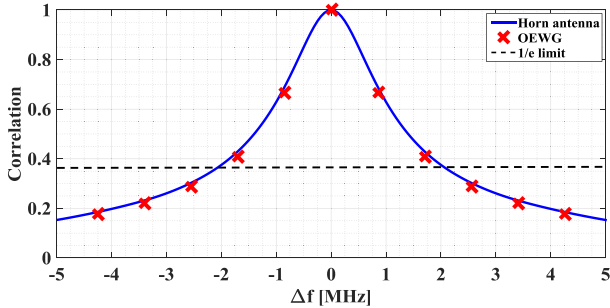


Fig. 7. Correlation of frequency samples averaged over all 10000 paddle orientations at antenna location number 5.

number of uncorrelated paddle orientations, is of utmost importance for the accurate estimation of the uncertainty and K factor.

The correlation of frequencies (coherence bandwidth) may be determined from the autocorrelation function (R) of the frequency-domain transfer function S_{21} [4], [9], [16]

$$R(\Delta f_i, n_i) = \sum_{j=1}^m S_{21}(f_j, n_i) S_{21}^*(f_j + \Delta f_i, n_i) \quad (8)$$

where $S_{21}(f, n)$ corresponds to the measured complex S_{21} at frequency step f_j with m frequency points measured within the bandwidth of interest, Δf corresponds to one of several frequency offsets over the bandwidth of interest, the index n_i is the mode-stirred sample (out of N), and the asterisk denotes complex conjugation.

The autocorrelation function was calculated in the frequency range from 43 to 47 GHz with 32001 frequency points for both the OEW and waveguide horn antennae. The results show a coherence bandwidth of ~ 4 MHz for a $1/e$ threshold [4], as shown in Fig. 7. This coherence bandwidth results in approximately 1000 uncorrelated frequency samples N_{fr} in the observed frequency range.

We next estimated the number of uncorrelated paddle orientations that the stirrers were able to provide. At each observed frequency, we determined whether the stirrer changed the boundary conditions to produce a statistically significant variation of the field distribution inside the chamber. Samples taken under statistically significant different conditions are considered uncorrelated.

In order to determine the number of uncorrelated paddle orientations, measurements were taken for 900 vertical stirrer orientations (0.4° paddle step), and the circular autocorrelation

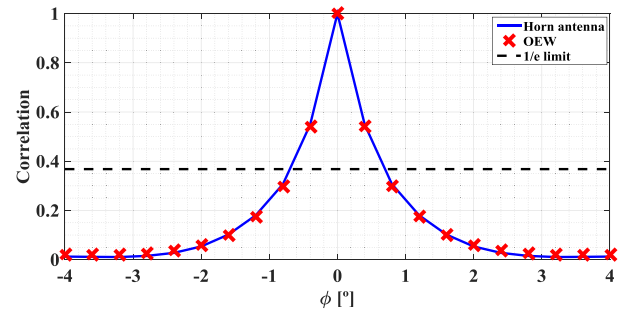


Fig. 8. Correlation between paddle orientations for a single vertical stirrer.

was computed [32] for both OEW and waveguide horn transmit antennae as

$$r = \frac{\langle S_{21n}(f_j) S_{21n+\Delta n}^*(f_j) \rangle_n - |\langle S_{21n}(f_j) \rangle_n|^2}{\langle |S_{21n}(f_j)|^2 \rangle_n - |\langle S_{21n}(f_j) \rangle_n|^2} \quad (9)$$

where we use the complex S_{21} -parameter at the j th frequency point f_j and n th stirrer orientation. The coherence angle (ϕ) obtained for a single vertical stirrer was $\sim 1.4^\circ$ for a $1/e$ threshold (Fig. 8). We use the coherence angle to estimate the total number of uncorrelated measurements (N_{est}) that may be achieved from a single stirrer [8], [33], [34] as $N_{est} = 360^\circ/\phi$. In our case, the calculated coherence angle would result in 257 uncorrelated measurements per stirrer, or a total of 66049 uncorrelated measurements for both the stirrers, assuming that both the stirrers can produce an equal number of uncorrelated samples per full turn.

A more accurate correlation metric may be found by taking into account the total amount of information (entropy) in the measured data [35]. Because correlation among measurements results in redundant information, the more correlated the measurement data, the lower the measurement data's overall entropy. Thus, one can determine an effective number of uncorrelated measurements (N_{eff}) for N potentially correlated measurements. For the sake of simplicity, we omit the complete derivation of the expression for calculating N_{eff} and the reader is referred to [35] for more details.

Prior work on finding the coherence angle and the number of the uncorrelated stirrer orientations can be found in [8], [26], [28], and [36]–[40]. In [35], we compared the entropy method to the other available methods with good agreement.

The effective number of uncorrelated measurements for the OEW and waveguide horn transmit antennae is shown in Fig. 9. N_{eff} calculated for 900 single stirrer orientations is presented by the solid line for the waveguide horn antenna and by the crosses for the OEW. N_{eff} converged to 260 with 1601 frequency points, which confirms the previously obtained N_{est} result, based on coherence angle. Good agreement was achieved, because we used a large sample size (900) to calculate the entropy. Note that entropy leads to the underestimation only if there are not enough measurement samples [40]–[42]. On the other hand, if the requirement for the sufficient sample size is met, the approach based on the entropy should yield similar results to the commonly used ($1/e$) approach. Entropy underestimation can also be

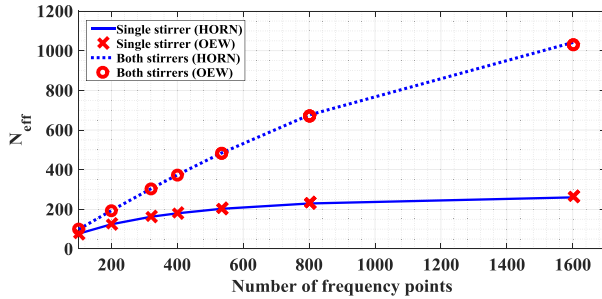


Fig. 9. Effective number of uncorrelated measurements N_{eff} for various transmit antennae for single and both stirrers at antenna location number 5.

minimized by applying correction terms [41], [42], which was beyond the scope of this paper. Instead, we only focused on the large number of measurement samples.

Note that we used 1601 frequencies even though the coherence bandwidth provided us with 1000 uncorrelated frequency samples. These additional frequency points add more information and improve our estimate, but are not used to calculate the uncertainty.

In addition, entropy may provide us the effective number of uncorrelated measurements that both stirrers can produce. For both the stirrers, the calculated N_{eff} was 1042 with 1601 frequency points. In Fig. 9, these results are presented by the dotted line for the waveguide horn antenna and circles for the OEW. However, direct estimation of the number of effective paddle orientations for both the stirrers (10000 physical paddle orientations) was not possible, as the number of uncorrelated frequency points in the observed frequency range was insufficient to achieve convergence.

B. K Factor

In RC measurements, the K factor is generally defined as the ratio of unstirred (P_u) and stirred power (P_s) and can be estimated from the S-parameters [13]

$$K = \frac{|\langle S_{21} \rangle_N|^2}{\langle |S_{21} - \langle S_{21} \rangle|^2 \rangle_N}. \quad (10)$$

The K factor depends on the antenna type, antenna position, and antenna orientation. In this paper, we studied the K factor with respect to different antenna types (waveguide horn antenna and OEW) and different locations (nine antenna locations). We did not study the effect of the antenna orientations due to the fact that we wanted to have the uncertainty as low as possible so we chose optimal antenna orientations (always aimed away from each other).

Note that (10) becomes rather inaccurate for small K factor values, e.g., when the stirred energy is several orders of magnitude larger than the unstirred energy [21], [44]. This is due to the fact that estimation is based on the mean of a distribution whose standard deviation is orders of magnitude higher than its mean. However, according to (6), in order to achieve the desired total uncertainty of 2%, it is necessary to have such low- K factor values.

To gain a basic understanding of this problem, a Monte Carlo simulation was utilized. The distribution

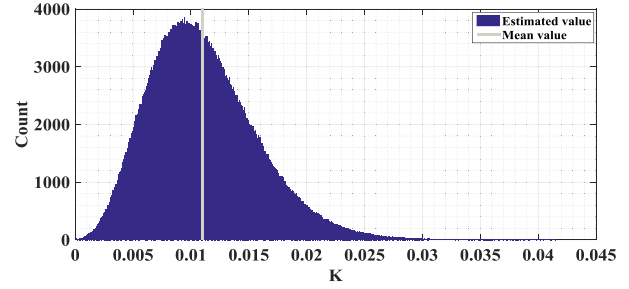


Fig. 10. Estimation of K factor from Monte Carlo simulation for a true K factor value of 0.01. The mean value was 0.011.

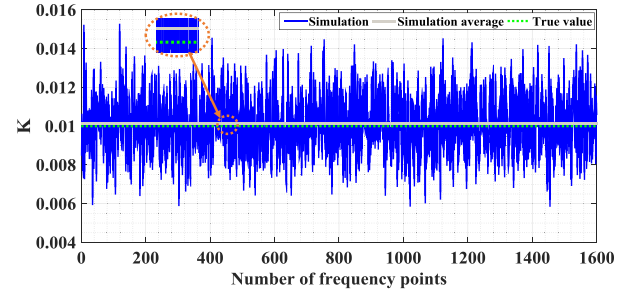


Fig. 11. K factor Monte Carlo simulation.

of K is shown in [21] to be $F(2, 2N - 2, 2N\kappa)/N$, where $F(2, 2N - 2, 2N\kappa)$ is a noncentral F distribution with 2 and $2N - 2$ degrees of freedom and noncentrality $2N\kappa$, where N is the number of uncorrelated mode-stirred samples [43] and κ is the K factor. A histogram based on 1600 random samples from this distribution is shown in Fig. 10. A true K factor of -20 dB was assumed, i.e., $\kappa = 0.01$ and $N = 10000$.

The distribution is asymmetric, making it more probable to overestimate the value of the K factor than to underestimate it. In addition, the mean of the distribution, found from Monte Carlo simulations, is not the true value 0.01, but 0.011, indicating the existence of underlying bias in the estimation.

The bias that arises from (10) was studied in [44], where a correction was derived

$$K_c = \frac{N - 2}{N - 1} \langle K \rangle_{N_{fr}} - \frac{1}{N}. \quad (11)$$

The first term in (11) introduces an almost negligible change for large N . However, $1/N$ represents a significant term for proper estimation of small K factors. In order to measure such small K factor values, a large number of uncorrelated measurement points should be available. If the K factor can be assumed as approximately constant for adjacent frequency points, K can then be averaged over the observed frequency range to obtain an improved estimate of the K factor, which is denoted by $\langle K \rangle_{N_{fr}}$, where N_{fr} is the number of uncorrelated frequency points. Monte Carlo simulation results using 1601 uncorrelated frequency points are shown in Fig. 11. The bias, given as the difference between the estimation of the K factor 0.011 (gray line) and its true value 0.01 (dotted cyan line), is clearly noticeable and indicates overestimation.

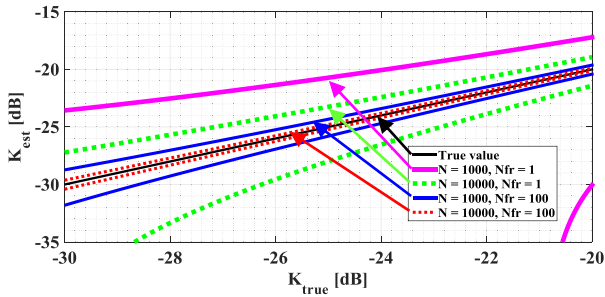


Fig. 12. 95% confidence intervals for the K factor based on different simulation scenarios.

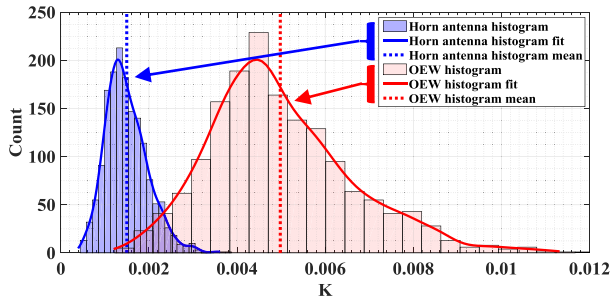


Fig. 13. Measured K factor data for the OEW and horn transmit antennae.

In addition, a 95% confidence interval, based on a large number of uncorrelated frequency points, was also proposed in [21]

$$\kappa_{2.5-97.5} = K_c \pm 1.96 \times \sqrt{\frac{(1 + \langle K \rangle_{N_{fr}})^2 + (N - 2)(1 + 2N \langle K \rangle_{N_{fr}})}{N^2(N - 3)N_{fr}}}. \quad (12)$$

The importance of frequency averaging is clearly shown in Fig. 12 where 95% confidence intervals, found from (12), were plotted for four different combinations of uncorrelated paddle orientations N and uncorrelated frequency points N_{fr} . Even 10000 uncorrelated paddle orientations are not sufficient to achieve a width of 95% confidence interval below 4 dB for a K_{true} of -28 dB without frequency averaging. Hence, in order to accurately estimate the K factor, both a sufficient number of uncorrelated paddle orientations and uncorrelated frequencies are required.

In order to achieve low uncertainty for TRP measurements, it is crucial to have an extremely low- K factor. Fig. 13 shows the measured K factor for all frequencies, for the OEW and waveguide horn transmit antennae. The red bars on the right present the histogram of the K factor for the OEW, while in the case of the horn transmit antenna, the results are presented by blue bars on the left. Since the OEW can be considered as a half-space omnidirectional antenna, its K factor, calculated from (10), is higher than that of the directional (waveguide horn) antenna. Note that the measured K factors of both the antennae are asymmetrical, such as that of the Monte Carlo simulation shown in Fig. 10. The uncorrected averaged K factor value for the waveguide horn

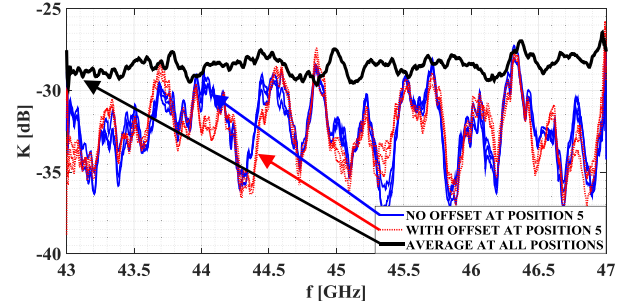


Fig. 14. Measurement repeatability with and without a paddle offset.

antenna was -28.25 and -23.03 dB for the OEW. By applying the correction given in (11), we obtain $K_c = -28.55$ dB for the waveguide horn antenna and -23.12 dB for the OEW.

An RC is often considered as a random environment where the specific DUT placement is not critical as long as enough independent samples are averaged for a specific location. However, the RC is, in fact, highly deterministic, meaning that measurements repeated in the same manner should yield similar results. We studied the repeatability of our K factor estimation by repeating three times the measurements of the waveguide horn antenna at position 5 (see Fig. 3) with and without an initial offset in the paddle angle. Three successive measurements were first performed for an initial stirrer angle of 0° with a 3.6° paddle step size. In Fig. 14, these measurements are presented by three solid lines. Afterward, three successive measurements were performed but now with an initial paddle angle of 1.8° , again with a 3.6° paddle step size. These results are presented by three dotted lines in Fig. 14. The results essentially show the chamber's performance in terms of the measurement repeatability (maximum difference 0.1%).

The drift of the measurement equipment and the repeatability of the paddles are shown by the differences between the same types of lines. Note the difference between the cluster of solid lines and the cluster of dotted lines indicates the uncertainty due to the finite number of uncorrelated paddle orientations. Variations in the K factor are significantly larger than our uncertainty, because the K factor is not constant inside the chamber, but varies with both frequency and position. However, averaging the data for different measurement antenna positions results in a more constant value across frequency, given by the black line in Fig. 14.

In some practical situations, it is impossible to access the antenna terminals on common wireless devices to determine the K factor. However, the proposed model still presents a good base for the setup where we can access the antenna terminals.

V. EVALUATION OF MEASUREMENT UNCERTAINTY

In Section II, theoretical expressions for measurement uncertainty due to the finite number of mode-stirred samples were discussed, and a significance test showed this component should reflect the RC setup uncertainty. One expression was based on the K factor and the other was derived directly from measurements of G_{REF} . The parameters necessary

TABLE II
K-FACTOR RESULTS AND MEASUREMENT UNCERTAINTY
ESTIMATED FROM (6) AND (7)

Antenna location	OEW		HORN	
	$K_{C,AVG}$ [dB]	$u_{REF,Kc}$ (6) [%]	$K_{C,AVG}$ [dB]	$u_{REF,Kc}$ (6) [%]
1	-23.41	1.1	-27.52	1.02
2	-22.53	1.14	-27.5	1.02
3	-23.12	1.11	-28.12	1.01
4	-23.07	1.11	-29.8	1.01
5	-24.11	1.07	-30.24	10.1
6	-22.72	1.13	-29.26	1.01
7	-23.12	1.11	-27.45	1.02
8	-22.94	1.12	-29.24	1.01
9	-23.21	1.11	-28.86	1.01
Pooled	-23.12	1.11	-28.55	1.01
Combined $u_{REF,Kc}$ (6) [%]	1.50			
u_{REF} (7) [%]	1.21		1.16	
Combined u_{REF} (7) [%]	1.68			

for evaluating these expressions were given in Section IV. The uncertainty observed in the actual measurements (7) will now be compared with the values predicted by the theoretical model (6) [11] where we used the corrected K factor, K_C , given by (11). The model proves to be accurate and highly useful for providing an estimation of the real measurement uncertainty for low- K environments.

Measurements performed at nine different antenna locations inside the chamber were used to form nine estimates of $\langle |S_{21}|^2 \rangle$, calculated for each of 1601 frequency points. This quantity was chosen, since it can be directly calculated from S-parameters measured by the VNA with no power calibration.

We compare the model for assessing the measurement uncertainty due to the finite number of mode-stirred samples given by (6) to an ideal chamber's uncertainty due to the finite number of mode-stirred samples. This can be calculated from [20]

$$u_{ideal} = \frac{1}{\sqrt{N}}. \quad (13)$$

Equation (13) gives us a theoretical lower bound on the uncertainty due to the finite number of mode-stirred samples under the assumption that the relative power measurements are identically exponentially distributed. This distribution implies that the real and imaginary components of the electric field may be represented by a zero-mean complex Gaussian distribution. For 10000 paddle orientations, the uncertainty due to the finite number of mode-stirred samples, calculated from (13), is 1%.

The estimated uncertainty at each antenna location, calculated from (6) for the OEW and horn transmit antennae, is given in Table II. $K_{C,AVG}$ represents the corrected K factor averaged over the observed frequency range. We compared the results from (6) and (7) and noticed excellent agreement ($\sim 0.07\%$ maximum difference). From Table II, we see that (6) estimates the pooled uncertainty for the DUT horn transmit antenna as 1.01% for a mean corrected K factor of -28.55 dB, while the uncertainty of 1%, based on an ideal chamber (13), was negligibly lower. However, even with

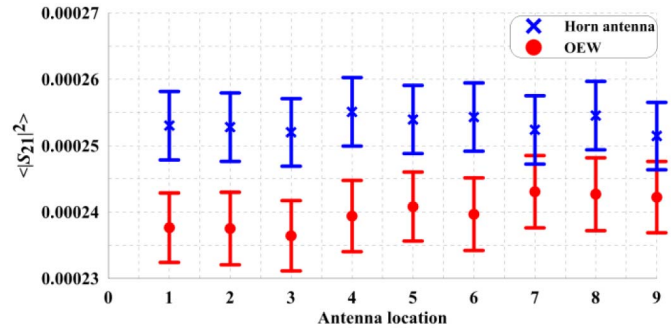


Fig. 15. Linear $\langle |S_{21}|^2 \rangle$ results at nine different antenna locations with expanded uncertainty error bars.

drift and repeatability effects present, we demonstrate that an uncertainty of $\sim 1\%$ is achievable.

By root-sum-of-squares combining the pooled uncertainty in the reference OEW and DUT (horn) measurements, we compute the random component of measurement uncertainty for TRP measurements as 1.50%, where the systematic effects are omitted. The combined measurement uncertainty for an ideal chamber is 1.4%, where it is assumed that an ideal chamber is equally excited, no matter which antenna is used. The calculated combined uncertainty obtained from (7) was 1.68% (see Table II), which was in good agreement with the combined uncertainty of 1.50% calculated from (6).

We show in Fig. 15 the measured values $\langle |S_{21}|^2 \rangle$ at nine different antenna locations with the expanded uncertainty ($\pm 2 \times u_{REF,Kc}$) from Table II for the waveguide horn antenna and the OEW. Since the expanded uncertainty error bars overlap for different antenna locations, we conclude that the component of the uncertainty due to the antenna location is not significant.

VI. CONCLUSION

The goal of this paper was to illustrate methods for obtaining low uncertainty at millimeter-wave frequencies. We reduced the uncertainty to $\sim 2\%$ by the use of mechanical paddle stirring and frequency stirring. A model for uncertainty estimation, based on a corrected K factor suitable for low-loss chamber setups, was compared with the ideal chamber uncertainty. This correction proved to be a useful and accurate tool for assessing measurement uncertainty.

The main parameters of this uncertainty estimator are the number of uncorrelated frequencies, the number of uncorrelated samples that the stirrer can produce, and the corrected K factor. The K factor depends on the directivities of the antennae used and their unstirred power coupling. While the stirred component depends on both the paddle and antenna stirring, the unstirred one only depends on antenna stirring.

A significance test was performed to compare the uncertainty due to the finite number of mode-stirred samples and the uncertainty due to the lack of spatial uniformity components. The outcome of the significance test allowed us to determine the correct expression for the standard uncertainty to use in our estimate of the total uncertainty. The uncertainty

due to the finite number of mode-stirred samples dominates for this low-loss setup.

The combined random component of the uncertainty due to the finite number of mode-stirred samples based on the corrected K factor was 1.5%. This was compared with the uncertainty in the ideal RC (1.4%) and with the uncertainty from the significance test (7) (1.68%), showing good agreement.

Since uncertainty at such high frequencies can play a vital role in RC measurements, these techniques can be used as a base point for future studies, which may include TRP measurements based on absolute power and modulated signals.

We also proposed some useful techniques to lower the measurement uncertainty for TRP measurements at millimeter-wave frequencies inside an electrically large RC. The millimeter-wave frequency range will be used in the next-generation, high-speed wireless networks, where measurement tolerances could be tight in future testing.

APPENDIX

In wireless tests, where chambers are often loaded, it is common that the uncertainty due to lack of spatial uniformity dominates, as compared with the uncertainty arising from the finite number of mode-stirred samples in a mode-stirring sequence [12]. However, for low-loss, high- Q setups, this is not always the case, and the relative effects of these two contributions should be studied. Therefore, we need to find the uncertainties associated with the number of mode-stirred samples N (10000 in our setup) and the spatial uniformity for M (nine in our setup) measurement antenna locations.

The mean squared deviation due to the mode-stirred samples is denoted by s_N^2 , while the mean squared deviation due to the lack of spatial uniformity is denoted by s_M^2 . Their values can be calculated as [12]

$$s_N^2 = \frac{1}{M(N-1)} \sum_{j=1}^M \sum_{i=1}^N [G_{\text{REF}}(n_i, m_j) - \langle G_{\text{REF}}(m_j) \rangle_N]^2 \quad (\text{A.1})$$

with $M(N-1)$ degrees of freedom and

$$s_M^2 = \frac{N}{M-1} \sum_{j=1}^M [\langle G_{\text{REF}}(m_j) \rangle_N - \langle G_{\text{REF}} \rangle_{N,M}]^2 \quad (\text{A.2})$$

with $M-1$ degrees of freedom. We write this deviation in terms of G_{REF} under the assumption that uncertainties in the antenna efficiencies do not contribute. The results for these two deviations are given in Table III.

To determine which of these two components for our chamber setup is dominant, a significance test may be used [12], [27]. The outcome of the significance test provides us with the correct expression for standard uncertainty in TRP measurements for a given chamber setup. The statistics for testing the significance of each uncertainty are based on an F distribution and given by [27]

$$F(s_M^2, s_N^2) = \frac{s_M^2}{s_N^2} \quad (\text{A.3})$$

TABLE III

SIGNIFICANCE TEST RESULTS AND COMPARISON WITH F DISTRIBUTION CONFIDENCE LEVELS

s_M^2	0.01*10⁻⁶
s_N^2	9.39*10⁻⁶
$F(s_M^2, s_N^2)$	0.001
$F_{0.90, n_1, n_2}$	1.67
$F_{0.95, n_1, n_2}$	1.94
$F_{0.99, n_1, n_2}$	2.51
u_{REF}	1.21%
u_{DUT}	1.16%
u_{COMB}	1.68%

with $M-1$ and $M(N-1)$ degrees of freedom. If the following holds:

$$F(s_M^2, s_N^2) < F_{0.95, M-1, M(N-1)} \quad (\text{A.4})$$

where F_{α, n_1, n_2} is the α quantile of the F distribution with n_1 and n_2 degrees of freedom, then the test is not significant.

The F distribution percentiles for the 90%, 95%, and 99% confidence levels, together with s_N^2 and s_M^2 and the results of the significance test, are given in Table III. The significance test results were smaller than the F distribution values for all confidence levels, indicating that the effect due to lack of spatial uniformity is not significant. Therefore, the standard uncertainty in the reference measurements can be calculated from

$$u_{\text{REF}} = \sqrt{\frac{\sum_{i=1}^N \sum_{j=1}^M [G_{\text{REF}}(n_i, m_j) - \langle G_{\text{REF}} \rangle_{N,M}]^2}{NM(NM-1)}}. \quad (\text{A.5})$$

The uncertainty in the DUT measurements is calculated from (A.5) by replacing G_{REF} with G_{DUT} . The reference (OEW), DUT (waveguide horn antenna), and combined standard uncertainty are given in Table III.

REFERENCES

- [1] M. L. Crawford and G. H. Koepke, "Design, evaluation, and use of a reverberation chamber for performing electromagnetic susceptibility/vulnerability measurements," U.S. Nat. Bureau Standards, Boulder, CO, USA, Tech. Note 1092, 1986.
- [2] D. A. Hill, "Electromagnetic theory of reverberation chambers," Nat. Inst. Standards Technol., Boulder, CO, USA, Tech. Note 1506, 1998.
- [3] *Requirements for the Control of Electromagnetic Interference Characteristics of Subsystems and Equipment*, document MIL-STD-461, U.S. Department of Defense, 1999.
- [4] *Electromagnetic Compatibility (EMC)—Part 4-21: Testing and Measurements Techniques—Reverberation Chamber Test Methods, Edition 2.0 2011-01*, document IEC 61000-4-21, 2005.
- [5] C. L. Holloway *et al.*, "Use of reverberation chambers to determine the shielding effectiveness of physically small, electrically large enclosures and cavities," *IEEE Trans. Electromagn. Compat.*, vol. 50, no. 4, pp. 770–782, Nov. 2008.
- [6] D. A. Hill, *Electromagnetic Fields in Cavities*. Piscataway, NJ, USA: Wiley, 2009.
- [7] C. L. Holloway, H. A. Shah, R. J. Pirkl, W. F. Young, D. A. Hill, and J. Ladbury, "Reverberation chamber techniques for determining the radiation and total efficiency of antennas," *IEEE Trans. Antennas Propag.*, vol. 60, no. 4, pp. 1758–1770, Apr. 2012.
- [8] K. Rosengren, P.-S. Kildal, C. Carlsson, and J. Carlsson, "Characterization of antennas for mobile and wireless terminals in reverberation chambers: Improved accuracy by platform stirring," *Microw. Opt. Technol. Lett.*, vol. 30, no. 6, pp. 391–397, Sep. 2001.

- [9] X. Chen, P.-S. Kildal, C. Orlenius, and J. Carlsson, "Channel sounding of loaded reverberation chamber for over-the-air testing of wireless devices: Coherence bandwidth versus average mode bandwidth and delay spread," *IEEE Antennas Wireless Propag. Lett.*, vol. 8, pp. 678–681, Jun. 2009.
- [10] P.-S. Kildal, X. Chen, C. Orlenius, M. Franzen, and C. L. Patané, "Characterization of reverberation chambers for OTA measurements of wireless devices: Physical formulations of channel matrix and new uncertainty formula," *IEEE Trans. Antennas Propag.*, vol. 60, no. 8, pp. 3875–3891, Aug. 2012.
- [11] K. A. Remley, R. J. Pirkl, H. A. Shah, and C.-M. Wang, "Uncertainty from choice of mode-stirring technique in reverberation-chamber measurements," *IEEE Trans. Electromagn. Compat.*, vol. 55, no. 6, pp. 1022–1030, Dec. 2013.
- [12] K. A. Remley, C.-M. J. Wang, D. F. Williams, J. J. van den Toorn, and C. L. Holloway, "A significance test for reverberation-chamber measurement uncertainty in total radiated power of wireless devices," *IEEE Trans. Electromagn. Compat.*, vol. 58, no. 1, pp. 207–219, Feb. 2016.
- [13] C. L. Holloway, D. A. Hill, J. M. Ladbury, P. F. Wilson, G. Koepke, and J. Coder, "On the use of reverberation chambers to simulate a Rician radio environment for the testing of wireless devices," *IEEE Trans. Antennas Propag.*, vol. 54, no. 11, pp. 3167–3177, Nov. 2006.
- [14] A. J. Pomianek, K. Staniec, and Z. Joskiewicz, "Practical remarks on measurement and simulation methods to emulate the wireless channel in the reverberation chamber," *Prog. Electromagn. Res.*, vol. 105, pp. 49–69, 2010.
- [15] P.-S. Kildal, C. Orlenius, and J. Carlsson, "OTA testing in multipath of antennas and wireless devices with MIMO and OFDM," *Proc. IEEE*, vol. 100, no. 7, pp. 2145–2157, Jul. 2012.
- [16] C. L. Holloway, H. A. Shah, R. J. Pirkl, K. A. Remley, D. A. Hill, and J. Ladbury, "Early time behavior in reverberation chambers and its effect on the relationships between coherence bandwidth, chamber decay time, RMS delay spread, and the chamber buildup time," *IEEE Trans. Electromagn. Compat.*, vol. 54, no. 4, pp. 714–725, Aug. 2012.
- [17] D. W. Matolak, K. A. Remley, C. Holloway, and C. Gentile, "Outdoor-to-indoor channel dispersion and power-delay profile models for the 700-MHz and 4.9-GHz bands," *IEEE Antennas Wireless Propag. Lett.*, vol. 15, pp. 441–443, Jul. 2015.
- [18] D. Kajfez, *Q Factor*, ISBN 0-930071-06-9. Oxford, U.K.: Vector Forum, 1994.
- [19] J. G. Kostas and B. Boverie, "Statistical model for a mode-stirred chamber," *IEEE Trans. Electromagn. Compat.*, vol. 33, no. 4, pp. 366–370, Nov. 1991.
- [20] X. Chen, P.-S. Kildal, and J. Carlsson, "Characterization and modeling of measurement uncertainty in a reverberation chamber with a rotating mode stirrer," in *Proc. EMC Europe*, Gothenburg, Sweden, Sep. 2014, pp. 296–300.
- [21] C. M. J. Wang *et al.*, "Parameter estimation and uncertainty evaluation in a low Rician K -factor reverberation-chamber environment," *IEEE Trans. Electromagn. Compat.*, vol. 56, no. 5, pp. 1002–1012, Oct. 2014.
- [22] P. Hallbjörner, U. Carlberg, K. Madsén, and J. Andersson, "Extracting electrical material parameters of electrically large dielectric objects from reverberation chamber measurements of absorption cross section," *IEEE Trans. Electromagn. Compat.*, vol. 47, no. 2, pp. 291–303, May 2005.
- [23] X. Zhou, J. Li, H. Fan, A. Bhohe, P. Sochoux, and J. Yu, "High-frequency EMC design verification through full-wave simulations and measurements in reverberation chamber," in *Proc. IEEE Int. Symp. EMC*, Denver, CO, USA, Aug. 2013, pp. 299–305.
- [24] A. K. Fall, P. Besnier, C. Lemoine, M. Zhadobov, and R. Sauleau, "Design and experimental validation of a mode-stirred reverberation chamber at millimeter waves," *IEEE Trans. Electromagn. Compat.*, vol. 57, no. 1, pp. 12–21, Feb. 2015.
- [25] C. Park and T. S. Rappaport, "Short-range wireless communications for next-generation networks: UWB, 60 GHz millimeter-wave WPAN, and ZigBee," *IEEE Trans. Wireless Commun.*, vol. 14, no. 4, pp. 70–78, Aug. 2007.
- [26] P. B. Papazian, K. A. Remley, C. Gentile, and N. Golmie, "Radio channel sounders for modeling mobile communications at 28 GHz, 60 GHz and 83 GHz," in *Proc. Global Symp. Millim. Waves (GSMM)*, Montreal, QC, Canada, May 2015, pp. 1–3.
- [27] Joint Committee for Guides in Metrology, "Evaluation of measurement data—Guide to the expression of uncertainty in measurement," Int. Bureau Weights Measures, Sèvres, France, Tech. Rep. 100:2008, Sep. 2008.
- [28] "Fundamentals of RF and microwave power measurements (part 1)," Agilent Technol., Santa Clara, CA, USA, Appl. Note 1449-1, Apr. 2003.
- [29] D. F. Williams. (Jun. 2014). NIST microwave uncertainty framework, beta version. NIST, Boulder, CO, USA. [Online]. Available: <http://www.nist.gov/ctl/rf-technology/related-software.cfm>
- [30] J. A. Jargon, D. F. Williams, T. M. Wallis, D. X. LeGolvan, and P. D. Hale, "Establishing traceability of an electronic calibration unit using the NIST microwave uncertainty framework," in *79th ARFTG Conf. Dig.*, Montreal, QC, Canada, Jun. 2012, pp. 1–5.
- [31] "De-embedding and embedding S-parameter networks using a vector network analyzer," Keysight Technol., Santa Rosa, CA, USA, Appl. Note 5980-2784EN, Jul. 2014.
- [32] K. G. Beauchamp and C. K. Yuen, *Digital Methods for Signal Analysis*. Sydney, NSW, Australia: George Allen & Unwin Ltd., 1976.
- [33] K. Madsén, P. Hallbjörner, and C. Orlenius, "Models for the number of independent samples in reverberation chamber measurements with mechanical, frequency, and combined stirring," *IEEE Antennas Wireless Propag. Lett.*, vol. 3, no. 1, pp. 48–51, Dec. 2004.
- [34] O. Lundén and M. Backström, "Stirrer efficiency in FOA reverberation chambers. Evaluation of correlation coefficients and chi-squared tests," in *Proc. IEEE Int. Symp. Electromagn. Compat.*, vol. 1, Aug. 2000, pp. 11–16.
- [35] R. J. Pirkl, K. A. Remley, and C. S. L. Patané, "Reverberation chamber measurement correlation," *IEEE Trans. Electromagn. Compat.*, vol. 54, no. 3, pp. 533–545, Jun. 2012.
- [36] J. Clegg, A. C. Marvin, J. F. Dawson, and S. J. Porter, "Optimization of stirrer designs in a reverberation chamber," *IEEE Trans. Electromagn. Compat.*, vol. 47, no. 4, pp. 824–832, Nov. 2005.
- [37] P. Hallbjörner, "Estimating the number of independent samples in reverberation chamber measurements from sample differences," *IEEE Trans. Electromagn. Compat.*, vol. 48, no. 2, pp. 354–358, May 2006.
- [38] C. Lemoine, P. Besnier, and M. Drissi, "Estimating the effective sample size to select independent measurements in a reverberation chamber," *IEEE Trans. Electromagn. Compat.*, vol. 50, no. 2, pp. 227–236, May 2008.
- [39] S. Pfennig and H. G. Krauthäuser, "A general method for determining the number of independent stirrer positions in reverberation chambers," in *Proc. Int. Symp. Electromagn. Compat. (EMC EUROPE)*, Rome, Italy, Sep. 2012, pp. 1–6.
- [40] S. Pfennig and H. G. Krauthäuser, "Comparison of methods for determining the number of independent stirrer positions in reverberation chambers," in *Proc. Int. Symp. Electromagn. Compat. (EMC EUROPE)*, Bruges, Belgium, Sep. 2013, pp. 431–436.
- [41] J. A. Bonachela, H. Hinrichsen, and M. Muñoz, "Entropy estimates of small data sets," *J. Phys. A, Math. Theor.*, vol. 41, no. 20, p. 202001, 2008.
- [42] P. Grassberger. (Feb. 2008). "Entropy estimates from insufficient samplings." [Online]. Available: <http://arxiv.org/abs/physics/0307138>
- [43] N. L. Johnson and S. Kotz, *Wiley Series in Probability and Mathematical Statistics: Distributions in Statistics*. New York, NY, USA: Wiley, 1970.
- [44] C. Lemoine, E. Amador, and P. Besnier, "On the K -factor estimation for Rician channel simulated in reverberation chamber," *IEEE Trans. Antennas Propag.*, vol. 59, no. 3, pp. 1003–1012, Mar. 2011.



Damir Senic (S'09–M'16) received the M.Sc. and Ph.D. degrees from the Faculty of Electrical Engineering, Mechanical Engineering and Naval Architecture, University of Split, Split, Croatia, in 2008 and 2014, respectively.

He is currently with the Communications Technology Laboratory, National Institute of Standards and Technology, University of Colorado at Boulder, Boulder, CO, USA, as a Postdoctoral Research Associate through the Professional Research Experience Program. His current research interests include millimeter wave radiocommunications, electromagnetic measurements, electromagnetic (EM) compatibility, and bioeffects of EM fields.

Dr. Senic received the Richard E. Merwin Award of the IEEE Computer Society for exemplary involvement in the IEEE activities and excellent academic achievement in 2013.



Kate A. Remley (S'92–M'99–SM'06–F'13) was born in Ann Arbor, MI, USA. She received the Ph.D. degree in electrical and computer engineering from Oregon State University, Corvallis, OR, USA, in 1999.

She was a Broadcast Engineer in Eugene, OR, USA, from 1983 to 1992, where she served as the Chief Engineer of an AM/FM broadcast station from 1989 to 1991. In 1999, she joined the RF Technology Division, National Institute of Standards and Technology (NIST), Boulder, CO, USA, as an Electronics Engineer. She is currently the Leader of the Metrology for Wireless Systems Group with NIST. Her current research interests include the development of calibrated measurements for microwave and millimeter-wave wireless systems, characterizing the link between nonlinear circuits and system performance, and developing standardized test methods for RF equipment used by the public-safety community.

Dr. Remley is a member of the Oregon State University Academy of Distinguished Engineers. She was a recipient of the Department of Commerce Bronze and Silver Medals and an ARFTG Best Paper Award. She was the Chair of the MTT-11 Technical Committee on Microwave Measurements from 2008 to 2010, and the Editor-in-Chief of the *IEEE Microwave Magazine* from 2009 to 2011, and is the Chair of the MTT Fellow Committee. She is a Distinguished Lecturer of the IEEE Electromagnetic Compatibility Society from 2016 to 2018.



Chih-Ming Jack Wang received the Ph.D. degree in statistics from Colorado State University, Fort Collins, CO, USA, in 1978.

He has been with the Statistical Engineering Division, National Institute of Standards and Technology, Boulder, CO, USA, since 1988. He has authored over 90 journal articles. His current research interests include statistical metrology and the application of statistical methods to physical sciences.

Dr. Wang is a fellow of the American Statistical Association (ASA). He is a recipient of the Department of Commerce Silver Medal, Bronze Medal, the NIST Allen V. Astin Measurement Science Award, and several awards from ASA.



Dylan F. Williams (M'80–SM'90–F'02) received the Ph.D. degree in electrical engineering from the University of California at Berkeley, Berkeley, CA, USA, in 1986.

He joined the Electromagnetic Fields Division, National Institute of Standards and Technology, Boulder, CO, USA, in 1989, where he develops electrical waveform and microwave metrology. He has authored over 100 technical papers.

Dr. Williams is a recipient of the Department of Commerce Bronze and Silver Medals, the Astin Measurement Science Award, two Electrical Engineering Laboratory's Outstanding Paper Awards, three Automatic RF Techniques Group (ARFTG) Best Paper Awards, the ARFTG Automated Measurements Technology Award, the IEEE Morris E. Leeds Award, the European Microwave Prize, and the 2013 IEEE Joseph F. Keithley Award. He served as an Editor of the *IEEE TRANSACTIONS ON MICROWAVE THEORY AND TECHNIQUES* from 2006 to 2010, and the Executive Editor of the *IEEE TRANSACTIONS ON TERAHERTZ SCIENCE AND TECHNOLOGY*. He is the President Elect of the IEEE Microwave Theory and Techniques Society.



Christopher L. Holloway (S'86–M'92–SM'04–F'10) received the B.S. degree from the University of Tennessee at Chattanooga, Chattanooga, TN, USA, in 1986, and the M.S. and Ph.D. degrees in electrical engineering from the University of Colorado at Boulder, Boulder, CO, USA, in 1988 and 1992, respectively.

He was a Research Scientist with Electro Magnetic Applications, Inc., Lakewood, CO, USA, in 1992. His responsibilities included theoretical analysis and finite-difference time-domain modeling of various electromagnetic problems. From 1992 to 1994, he was with the National Center for Atmospheric Research, Boulder, where he was involved in wave propagation modeling, signal processing studies, and radar systems design. From 1994 to 2000, he was with the U.S. Department of Commerce Boulder, Institute for Telecommunication Sciences, Boulder, where he was involved in wave propagation studies. Since 2000, he has been with the National Institute of Standards and Technology, Boulder, where he has been involved in electromagnetic theory. He is currently a Graduate Faculty Member with the University of Colorado at Boulder. His current research interests include electromagnetic field theory, wave propagation, guided wave structures, remote sensing, numerical methods, metamaterials, measurement techniques, electromagnetic compatibility (EMC)/electromagnetic interference issues, and atom-based metrology.

Dr. Holloway is a member of the URSI Commissions A, B, and E. He was an Associate Editor of the *IEEE TRANSACTIONS ON EMC*. He was the Chairman of the Technical Committee on Computational Electromagnetics (TC-9) of the IEEE EMC Society from 2000 to 2005. He served as the Co-Chair of the Technical Committee on Nano-Technology and Advanced Materials (TC-11) of the IEEE EMC Society from 2006 to 2011. He is serving as the Chair of the U.S. Commission A of the International Union of Radio Science. He also served as the IEEE Distinguished Lecturer of the EMC Society from 2004 to 2006.



Diogo C. Ribeiro (S'09) was born in Portugal. He received the M.Sc. degree in electronics and telecommunications engineering from the University of Aveiro, Aveiro, Portugal, in 2011, where he is currently pursuing the Ph.D. degree.

He was a Guest Researcher with the National Institute of Standard and Technology, Boulder, CO, USA, in 2015. He is currently with the Telecommunications Institute (IT), University of Aveiro, Lisboa, Portugal. His current research interests include software-defined radio measurements and mixed-signal characterization. The research topic covered during the project was the measurement and pre-correction of traceable wideband millimeter wave sources and the analysis of associated uncertainty.

Mr. Ribeiro received the Best Student Paper Award 2012 at the Sixth Congress of Portuguese Committee of URSI, the second prize in the IMS2013 Measurement Student Design Competition, and the second prize in the IMS2015 LSNA Round Robin Student Design Competition. He was a recipient of the 2016 ARFTG Roger Pollard Memorial Student Fellowship in Microwave Measurements.



Ansgar T. Kirk was born in Osnabrück, Germany. He received the M.Sc. degree in mechatronics from the Leibniz Universität Hannover, Hanover, Germany, in 2013, where he is currently pursuing the Dr.-Ing. degree in electrical engineering.

He was a Guest Researcher with the Electromagnetics Division, National Institute of Standards and Technology, Boulder, CO, USA, from 2012 to 2013, where he was involved in low-uncertainty measurements in reverberation chambers for wireless devices. He is currently a Research Engineer with the Institute of Electrical Engineering and Measurement Technology, Leibniz Universität Hannover. His current research interests include ultrahigh resolution ion mobility spectrometers and the required specialized electronics for them.